The 10th International Conference on Modeling and Diagnostics for Advanced Engine Systems (COMODIA 2022), July 5-8, 2022, Sapporo, Japan

<10>

Improved Correlations for the Unstretched Laminar Flame Properties of Iso-Octane/Air Mixtures

*Delong Li, Ron Matthews, and Matt Hall

Department of Mechanical Engineering, The University of Texas
405 East Dean Keeton, Austin, TX 78712, USA

Key Words: Combustion, Modeling, Laminar Flame

ABSTRACT

The unstretched laminar flame speed (LFS) plays a key role in engine models and predictions of flame propagation. It is also an essential parameter in the study of turbulent combustion and can be directly used in many turbulent combustion models. Therefore, it is important to predict the laminar flame speed accurately and efficiently. Two improved correlations for the unstretched laminar flame speed, namely improved power law and improved Arrhenius form correlations, are proposed for iso-octane/air mixtures in this study, using simulated results for typical operating conditions for spark-ignition engines: unburned temperatures of 300-950 K, pressures of 1-120 bar, and equivalence ratios of 0.6-1.5. The original data points used to develop the new correlations were obtained using the detailed combustion kinetics for iso-octane from Lawrence Livermore National Laboratory (LLNL). The three coefficients in the improved power law correlation were determined using a methodology different from previous approaches. The improved Arrhenius form correlation employs a function of unburned gas temperature to replace the flame temperature, making the expression briefer and making the coefficients easier to calculate. The improved Arrhenius method is able to predict the trends and the values of laminar flame speed with improved accuracy over a larger range of operating conditions. The improved power law method also works well but for a relatively narrow range of predictions. The improved Arrhenius method is recommended, considering its overall fitting error was only half of that using the improved power law correlation and it was closer to the experimental measurements. Even though ϕ_m, the equivalence ratio at which the laminar flame speed reaches its maximum, is not monotonic with pressure, this dependence is still included, since it produces least-rich best torque (LBT). The comparisons between the improved correlations in this study and the experimental measurements and the other correlations from various researchers are shown as well.

INTRODUCTION

The unstretched laminar flame speed is a thermochemical property of a premixed reactive mixture, defined as the flame propagation speed normal to the flame surface. It is one of the most important parameters in flame chemistry, and can be used in many areas, including engine design and fundamental research. Many turbulent combustion models also rely on the laminar flame speed to calculate the turbulent burning velocity, and therefore can predict the overall performance of an engine. The fractal engine simulation model [1,2], for example, studied the effects of flame wrinkling and stretch caused by turbulence in spark-ignition (SI) engines, and introduced the fractional surface area increase factor to predict the turbulent mass burning rate calculated from the laminar flame speed. Therefore, many studies have been dedicated to obtaining accurate laminar flame speeds at different conditions and correlating the results to simple expressions for practical use.

The unstretched laminar flame speed depends upon the composition of the reactants (including the fuel type, equivalence ratio, and the diluents), the unburned temperature, and the system pressure. It can be determined by experiments, using a variety of techniques [3]. The laminar flame speed can also be predicted numerically, using chemical kinetics (e.g.: [4,5]). Based on these results, different correlations were proposed to predict the laminar flame speed at different conditions.

Perhaps the most widely used of these was developed by Metghalchi and Keck [6,7]. They used a power law form of equation to represent laminar flame speed (shown in Eqn. (1) and Eqn. (2)), based on the measurements for different fuels, including propane, methanol, iso-octane, and indolene (the gasoline used for emissions and fuel economy certification at the time).

$$S_L = S_{L0}\left(\frac{T_u}{T_0}\right)^{\alpha}\left(\frac{p}{p_0}\right)^{\beta} f_d \quad (1)$$

$$f_d = 1 - 2.1f \quad (2)$$

where S_{Lo} is the unstretched laminar flame speed at the baseline temperature and pressure (T_o and p_o), α and β are fuel and equivalence ratio dependent coefficients; and f_d is a factor to include the effects of diluent, and f is the diluent mass fraction. They showed S_{Lo} as a simple parabolic function of equivalence ratio, with α and β as linear functions of equivalence ratio, based on their measurements.

Many other studies also employed the same power law form of expression (Eqn. (1)) in their correlations. Bozza et al. [8] used a more complicated form (Eqn. (3)), a 4th order polynomial equation, to denote S_{Lo}, and used a function (Eqn. (4)) of both diluent mass fraction and equivalence ratio for the diluent dependence term, based on their one-dimensional simulation results employing CHEMKIN.

$$S_{L0} = A + B\phi + C\phi^2 + D\phi^3 + E\phi^4 \quad (3)$$

$$f_d = (1 - \kappa f)^{\gamma_1 + \gamma_2 \phi} \quad (4)$$

where A-E have linear correlations with fuel sensitivity, the difference between the Research Octane Number (RON) and the Motor Octane Number (MON); κ, γ_1, and γ_2 are parameters determined by regression. This correlation seemed more complicated, but still used a function of polynomial form to represent S_{Lo}.

Still based on the power law correlation, d'Adamo et al. [9] used a form of fifth order logarithmic polynomial as the fitting function, shown in Eqn. (5).

$$S_L = \left[\sum_{i=0}^{5} a_i \log(\phi)^i\right] * \left(\frac{T}{T_0}\right)^{\sum_{i=0}^{5} b_i \log(\phi)^i} * \left(\frac{p}{p_0}\right)^{\sum_{i=0}^{5} c_i \log(\phi)^i} \quad (5)$$

D'Adamo et al. determined a_i, b_i, and c_i for different fuels, including gasoline, iso-octane, n-heptane, and toluene, based on their one-dimensional simulation results at different conditions.

A different method from the power law form was shown by Lavoie [10]:

$$(1 - f)V_{STP} = A * p^n * e^{-\frac{E}{2RT_f}} \quad (6)$$

where V_{STP} is the flame speed, normalized in terms of mass flow rate, at standard conditions and A and E are functions of equivalence ratio. Lavoie used 0.8 for n, determined for stoichiometric conditions. This method proposed a semi-empirical correlation of Arrhenius form for the laminar flame speed and matched well with existing data.

Also in Arrhenius form, a more simplified version was proposed by Ryan and Lestz [11]:

$$S_L = b_1 * p^{b_2} * e^{-\frac{b_3}{T_u}} \quad (7)$$

where b_1, b_2, and b_3 are different constants for different fuels and equivalence ratios.

Correlations for S_{Lo} in other forms have also been proposed [12,13].

As seen above, various correlations for the unstretched laminar flame speed have been proposed for a variety of fuels. However, it is very difficult to have a simple correlation that produces excellent predictions over a wide range of operating conditions. For instance, Metghalchi and Keck [7] had a very simple function for the coefficients in the power law expression, but it was derived from only three equivalence ratios at ϕ = 0.8, 1.0, and 1.2, and might not be applicable outside this range. D'Adamo's correlations covered a wide range of engine conditions based on their 1-D kinetics results [9], but they had to use a complicated expression, a fifth order logarithmic polynomial, in their correlation.

In the present paper, two improved correlations are proposed to predict laminar flame speeds over the typical operating conditions for a SI engine. All the correlations were based on one-dimensional simulation results, to get multiple data points over the ranges of interest. The standard errors for the curve fits are reported to show the fitting quality and to compare the two improved methods. ϕ_m and LFS_m were investigated, and the correlations for both are provided. Validations and comparisons with experimental measurements from other studies are made as well.

METHODOLOGY

All the conditions, with different temperatures, pressures, and equivalence ratios, were simulated using CONVERGE CFD™ (CONVERGE below for short), a commercial computational fluid dynamics (CFD) package widely used in engine simulations and chemically reacting flow calculations. The CONVERGE one-dimensional premixed model was used to produce the laminar freely propagating flame speeds. A detailed chemical kinetics mechanism [14,15] for iso-octane, the latest version published by Lawrence Livermore National Laboratory (LLNL) and developed based on the mechanism of Curran et al. [16], was used in the simulations. It included 874 species and 3796 reactions, and was validated against experimental measurements over a wide range of temperatures and pressures. All the simulated laminar flame speed results were analyzed and fit to different equations using the codes in Python.

RESULTS

Simulation Results

Considering the typical operating cycles for an engine, different conditions were simulated, including an unburned temperature range from 300 K to 950 K, a pressure range from 1 bar to 120 bar, and an equivalence ratio range from 0.6 to 1.5. From the simulated results it was found that the flame speed increases with temperature while decreases with pressure for iso-octane and peaks somewhere between an equivalence ratio of 1.0 and 1.2.

Correlations for ϕ_m and LFS_m

ϕ_m refers to the equivalence ratio at which laminar flame speed reaches the maximum for a given temperature and pressure, and accordingly, LFS_m is the laminar flame speed value at ϕ_m. It will be useful to know ϕ_m and LFS_m, and both values will provide invaluable information, especially since ϕ_m should correspond to least-rich best torque (LBT). ϕ_m is in the range of 1.0 to 1.2 for iso-octane. To get more accurate results, more cases were simulated with a step of equivalence ratio of 0.01 within a range from 1.00 to 1.20.

ϕ_m results are shown in Fig. 1 first, where the horizontal axis represents the pressure and different curves show the dependencies on unburned temperature. It has to be emphasized that the accuracy for ϕ_m is 0.01, limited by the simulated step of equivalence ratio, so these curves are not smooth. ϕ_m values fall within a narrow range around 1.10 and increase monotonically with temperature (the same trend would be seen if all values at different simulated temperatures were plotted). However, ϕ_m decreases with pressure first and then increases again

when the system pressure is very high.

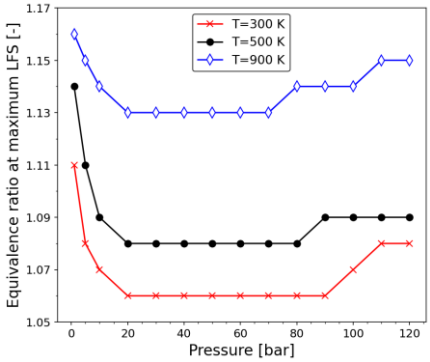

Fig. 1 ϕ_m value at different pressures: blue, temperature fixed at 900 K; black, temperature fixed at 500 K; red, temperature fixed at 300 K.

A correlation is proposed to show the estimation for the value of ϕ_m. Considering the limited accuracy of ϕ_m and the non-monotonic behavior with a large range of pressure, the correlation in this study only focuses on the low-pressure range. To present better predictions, more cases were simulated for the pressure range 1-12 bar with a step of 1 bar and temperature range 300-750 K with a step of 50 K. The correlation is shown in Eqn. (8).

$$\phi_m = A * \left(\frac{T_u}{T_0} + B\right) * \left[\left(\frac{p}{p_0}\right)^2 + C\left(\frac{p}{p_0}\right) + D\right] \quad (8)$$

where T_o = 298.15 K and p_o = 1 atm (to be consistent with Metghalchi and Keck [7]); four constants: A, 1.5243e-5; B, 28.576; C, -23.051; D, 2494.5. Again, this correlation could predict ϕ_m with a precision of 0.01, and could clearly present the trends with temperature and pressure for the conditions shown above. We will attempt to obtain a better correlation for the full ranges of T and P by the time this paper is presented.

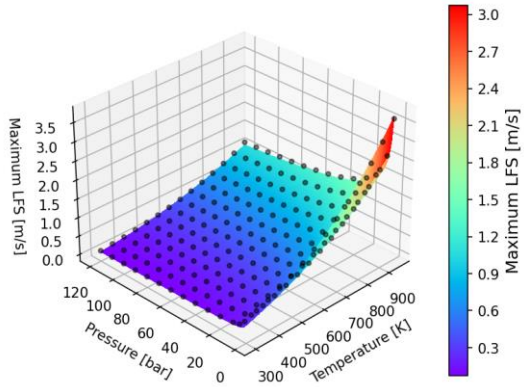

Fig. 2 Effects of temperature and pressure on LFS_m, the maximum unstretched laminar flame speed; black dots are the results from the LLNL detailed kinetics scheme for iso-octane, and the color maps are the fitted correlation.

The LFS_m results are shown in Fig. 2, where each black dot corresponds to one value at one temperature and pressure. Since ϕ_m at different temperatures and pressures are almost in the same range, LFS_m also follows the power law correlations. Therefore, all the results are fitted based on the equation shown in Eqn. (9) and the corresponding coefficients are shown in Table 1.

$$LFS_m = LFS_0 * \left(\frac{T_u}{T_0}\right)^{\alpha} * \left(\frac{p}{p_0}\right)^{\beta} \quad (9)$$

Table 1 Coefficients in Eqn. (9) for LFS_m of iso-octane in the unit of m/s.

LFS_o [m/s]	α	β
0.2344	2.3654	-0.2561

The color maps shown in Fig. 2 were generated based on the fitted expression, and they are very close to the original simulation points.

Correlations for Laminar Flame Speed with Temperature, Pressure, and Equivalence Ratio

Improved Power Law Form

The basic power law correlations have the same forms as Eqn. (10) shown in Metghalchi and Keck's papers [6,7]. However, the expressions used to derive the three terms (S_{Lo}, α, and β) are different in the present study.

$$S_L = S_{L0} * \left(\frac{T_u}{T_0}\right)^{\alpha} * \left(\frac{p}{p_0}\right)^{\beta} \quad (10)$$

where T_o = 298.15 K and p_o = 1 atm (1.01325 bar) are used as the reference temperature and pressure in this study to be consistent with Metghalchi and Keck; S_{Lo}, α, and β are three coefficients that are dependent on the fuel (i-octane in the present case) and equivalence ratio. In particular, S_{Lo} is the unstretched laminar flame speed at the reference temperature T_o and the reference pressure p_o.

The simulated S_{Lo} and the curve fits for S_{Lo} are shown in Fig. 3, as red crosses and the black dashed curve, respectively. To achieve more accurate curve fits around ϕ_m, an equivalence ratio step of 0.01 was used for the range of 1.0-1.2, while a step of 0.05 was used for other ranges. That is why denser points can be seen around ϕ_m in Fig. 3. Two parabolic formulas were used for the curve fits of S_{Lo}, as shown in Eqn. (11), to reflect the different LFS trends shown on the leaner side ($\phi < \phi_m$) and the richer side ($\phi > \phi_m$). Note that all the coefficients of the curve fits in this study are denoted in capital letters to better distinguish from the constants α and β in the S_L equations.

$$S_{L0} = \begin{cases} S_{L0_1}: A_0\phi^2 + B_0\phi + C_0, when\ \phi < \phi_m \\ S_{L0_2}: A_1\phi^2 + B_1\phi + C_1, when\ \phi > \phi_m \end{cases} \quad (11)$$

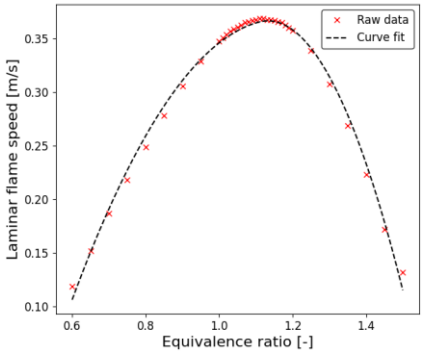

Fig. 3 Fitted results for laminar flame speed at reference temperature and pressure.

To make the two parabolic curves continuous and smooth at ϕ_m, two constraints were applied, shown in Eqn. (12).

$$\begin{cases} S_{L0_1}(\phi_m) = S_{L0_2}(\phi_m) \\ S_{L0_1}{}'(\phi_m) = S_{L0_2}{}'(\phi_m) \end{cases} \quad (12)$$

The three fitted coefficients for each case for iso-octane are given in Table 2.

Table 2 Coefficients in Eqn. (11) (A denotes A_0 when $\phi < \phi_m$, and denotes A_1 when $\phi > \phi_m$; the same for B & C) for laminar flame speed fits (m/s) at 298.15 K and 1 atm: ϕ_m =1.12.

Equivalence ratio	A	B	C
$\phi < \phi_m$	-0.8478	1.9590	-0.7648
$\phi > \phi_m$	-1.8957	4.3063	-2.0793

Based on the curve fit results for S_{Lo}, the other two parameters (α and β) in Eqn. (10) can be obtained at different equivalence ratios. The values for α and β, as well as the curve fits as a function of equivalence ratio, are shown in Fig. 4 and Fig. 5.

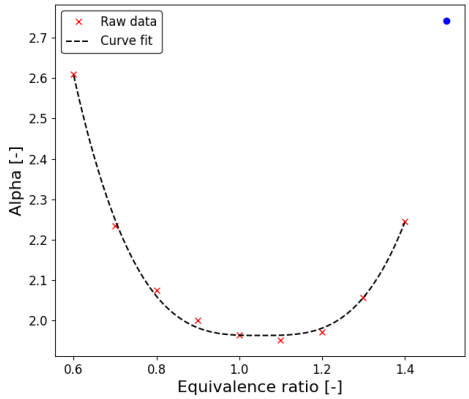

Fig. 4 Fitted results for α as a function of equivalence ratio, the blue dot represents the α value at an equivalence ratio of 1.5.

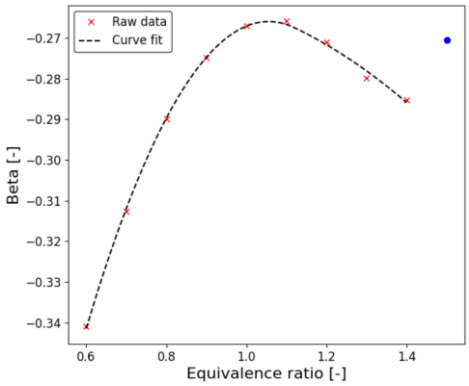

Fig. 5 Fitted results for β as a function of equivalence ratio: the blue dot represents the β value at an equivalence ratio of 1.5.

Eqn. (13) was used to represent coefficient α.

$$\alpha = A|\phi - B|^C + D \quad (13)$$

The coefficient β was fit by two continuous parabolic expressions shown in Eqn. (14), similar to what was shown for S_{Lo} to consider the different trends on the leaner and richer sides.

$$\beta = \begin{cases} A_0\phi^2 + B_0\phi + C_0, when\ \phi < \phi_m \\ A_1\phi^2 + B_1\phi + C_1, when\ \phi > \phi_m \end{cases} \quad (14)$$

It is worth noting that the above fits for α and β were applied for the equivalence ratio range from 0.6 to 1.4. The values for the very rich mixture at ϕ =1.5, shown as the blue dots in Fig. 4 and Fig. 5, deviated from the trends of the others. Different correlations for α and β should exist for the very rich region, which are not covered in this research. Therefore, the values at ϕ=1.5 are not included in all the following fits and discussions, and all the results shown below will work only for the equivalence ratio range 0.6-1.4.

The fit coefficients in Eqns. (13) and (14) are provided in Table 3.

Table 3 Coefficients for α (Eqn. (13)) and β (Eqn. (14)) (A denotes A_0 when $\phi < \phi_m$, and denotes A_1 when $\phi > \phi_m$; the same for B & C) for laminar flame speed fits (m/s) using the improved power law method: ϕ_m =1.12.

coefficients	A	B	C	D
α	8.4004	1.0513	3.2306	1.9634
β	A	B	C	
	$\phi < \phi_m$			
	-0.3639	0.7681	-0.6713	
	$\phi > \phi_m$			
	-0.0666	0.1021	-0.2984	

The power law form correlations are compared with the original data points in Fig. 6, where the unburned temperature is fixed at 950 K and the horizontal axis represents different pressures, and Fig. 7, where the pressure is fixed at 100 bar and the horizontal axis represents different unburned temperatures. In both figures, the curves with different colors show the equivalence ratio dependencies. Surprisingly, the predicted results using the power law correlations seem to deviate from the original data points to some extent. The predicted curves at 950 K shown in Fig. 6 present the similar trend of laminar flame speed with the original simulated results, whereas the values are consistently lower. This is also indicated in Fig. 7 showing the temperature dependence, where for all equivalence ratios, the predicted flame speeds are lower for the temperatures larger than 850 K, while higher for the lower temperature range. It could be concluded that the power law form is appropriate to express the pressure dependence, while the power law relation has to be replaced or expanded to express the temperature dependence over such a wide range of conditions.

In spite of failing to predict the laminar flame speeds very accurately in this part, the power law form can still be used for a relatively narrow range of temperatures and pressures, which will be shown in the "Discussion" section.

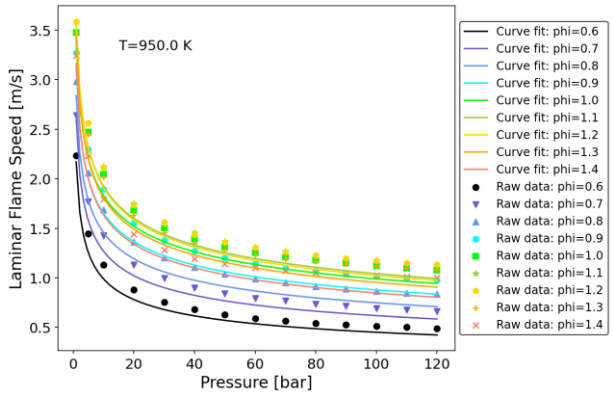

Fig. 6 Predicted laminar flame speeds using the improved power law correlations with different pressures and equivalence ratios at 950 K: curves for correlations and points for simulated results.

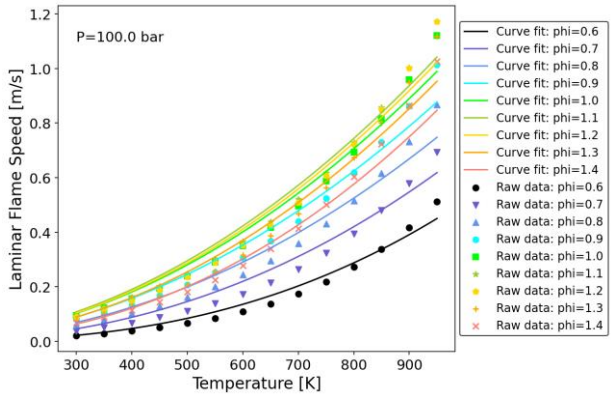

Fig. 7 Predicted laminar flame speeds using the improved power law correlations with different temperatures and equivalence ratios at 100 bar: curves for correlations and points for simulated results.

Improved Arrhenius Form

The power law form correlation is expanded in this section into the improved Arrhenius relation, based on Lavoie's semi-empirical correlation (Eqn. (15)), derived in reference [10] based on Zeldovich, Frank-Kamenetsky, and Semenov's theory [17] of laminar flame propagation to correlate the data obtained from previous experimental measurements.

$$V_{STP} \equiv \frac{\rho_u S_L}{\rho_{STP}} = a * p^n * \exp\left(-\frac{E}{2RT_f}\right) \qquad (15)$$

where V_{STP} is the mass average burning velocity, converted to the standard conditions; a, the pre-exponential factor and E, the activation energy are only functions of equivalence ratio and fuel; R is the gas constant, p is the pressure in atmospheres; and T_f is the flame temperature.

Then the unburned temperature, T_u, is introduced using the ideal gas law to eliminate the density terms, and Eqn. (15) can be rearranged in the form of Eqn. (16), which was also shown in Metghalchi and Keck's paper [7].

$$S_L = U\left(\frac{T_u}{T_0}\right)\left(\frac{p}{p_0}\right)^{\alpha} \exp\left(-\frac{\beta}{T_f}\right) \qquad (16)$$

where T_o=298.15 K and p_o=1 atm are the reference temperature and pressure; U is the pre-exponential factor; α and β are the coefficients to be determined as a function of equivalence ratio for iso-octane. Note for the pressure dependence power n in Eqn. (15), Lavoie used a constant value, determined for ϕ=1, for all the equivalence ratios. However, it is shown later in the present paper that the pressure dependence parameter is also a function of ϕ.

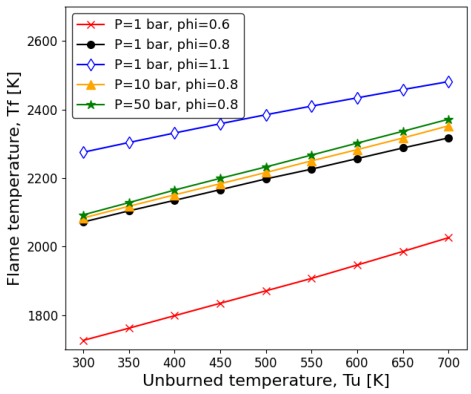

Fig. 8 Simulated results for the flame temperatures of iso-octane at different conditions (red crosses: p=1 bar and ϕ=0.6; black dots: p=1 bar and ϕ=0.8; blue diamonds: p=1 bar and ϕ=1.1; green stars: p=50 bar and ϕ=0.8; orange triangles: p=10 bar and ϕ=0.8).

A new term was added to the power law form that is a function of T_f; this term adds additional complexity to the calculation. However, it is noted that T_f, is a strong function of the unburned gas temperature and equivalence ratio, but a very weak function of pressure. Fig. 8 shows the simulated results for T_f, as a function of unburned gas temperature, pressure, and equivalence ratio. For the same ϕ, T_f has a linear correlation with T_u, and when ϕ changes, T_f differs a lot due to the combustion chemistry. For the three conditions at ϕ =0.8, the T_f values at the same T_u are very close, even though the pressure changes from 1 bar to 50 bar. Thus, it is concluded that in Eqn. (17) that for the same ϕ, T_f can be represented by a function of T_u.

$$T_f = kT_u + \gamma \qquad (17)$$

where k and γ are two coefficients to be determined. Combining Eqns. (16) and (17), the S_L correlation becomes:

$$S_L = U\left(\frac{T_u}{T_0}\right)\left(\frac{p}{p_0}\right)^{\alpha} \exp\left(-\frac{\beta/k}{T_u + \gamma/k}\right) \qquad (18)$$

or

$$S_L = U\left(\frac{T_u}{T_0}\right)\left(\frac{p}{p_0}\right)^{\alpha} \exp\left(-\frac{\beta'}{T_u + \gamma'}\right) \qquad (19)$$

For simplicity, β and γ are now redefined as β' and γ', respectively, to yield:

$$S_L = U\left(\frac{T_u}{T_0}\right)\left(\frac{p}{p_0}\right)^{\alpha} \exp\left(-\frac{\beta}{T_u + \gamma}\right) \qquad (20)$$

where U, α, β, and γ are functions of only equivalence ratio for iso-octane.

The four coefficients in Eqn. (20) can be obtained by correlating all of the LFS results from the simulations.

The values at different equivalence ratios are shown in Fig. 9, where the red dots are the fitted values for different coefficients at different equivalence ratios, and the black curves shown in Fig. 9b-d are the curve fits as a function of equivalence ratio.

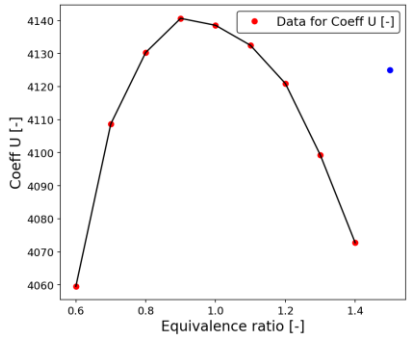

(a)

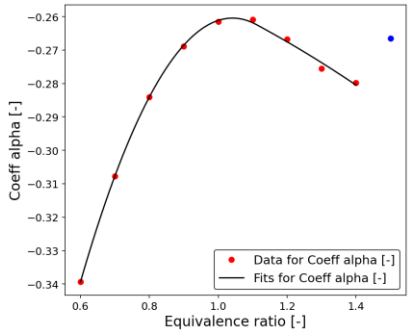

(b)

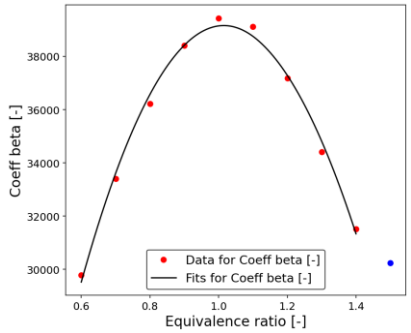

(c)

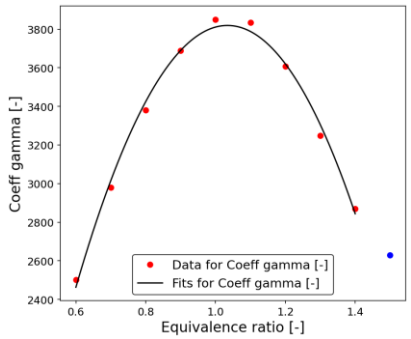

(d)

Fig. 9 Four coefficients in the improved Arrhenius form fits (Eqn. (20)) as a function of equivalence ratio and the fitted results: coefficient U (no fitting applied) in (a), α in (b), β in (c) and γ in (d); the blue dots represent the values at ϕ=1.5.

As seen in Fig. 9a, the data points for the pre-exponential factor, U, fall within the approximate range 4060-4140, and use of the average value produces only a 1% error in calculating the laminar flame speed, which is negligible, so there is no need to generate a fit for U. A piecewise 2nd order polynomial equation (Eqn. (21)), also shown earlier, was used to fit each of the other three coefficients as a function of ϕ, which are presented in Fig. 9b-d.

$$coeff = \begin{cases} A_0\phi^2 + B_0\phi + C_0, when\ \phi < \phi_m \\ A_1\phi^2 + B_1\phi + C_1, when\ \phi > \phi_m \end{cases} \quad (21)$$

In conclusion, the improved Arrhenius form correlation is presented in Eqn. (22), and the coefficients used in the 2nd order polynomial fit (Eqn. (21)) to get α, β, and γ are summarized in Table 4.

$$S_L = 4100\left(\frac{T_u}{T_0}\right)\left(\frac{p}{p_0}\right)^{\alpha} \exp\left(-\frac{\beta}{T_u+\gamma}\right) \quad (22)$$

Table 4 Coefficients (A denotes A_0 when $\phi < \phi_m$, and denotes A_1 when $\phi > \phi_m$; the same for B & C) for α, β, and γ in the improved Arrhenius form correlations (Eqn. (21)).

coefficient	ϕ_m=1.12	A	B	C
α	$\phi < \phi_m$	-0.4017	0.8385	-0.6978
β		-56127	113882	-18604
γ		-7228	14939	-3899
α*100	$\phi > \phi_m$	-0.6462	-4.6965	-20.1954
β		-49374	98754	-10132
γ		-7259	15007	-3938

The predicted laminar flame speeds using the improved Arrhenius form correlations, as well as the original simulated values from the detailed kinetics calculations, are shown in Fig. 10 and Fig. 11. Compared to the improved power law form, the improved Arrhenius form correlation works quite well under a wide range of conditions. The standard deviations for the fits will be shown in the "Discussion" section.

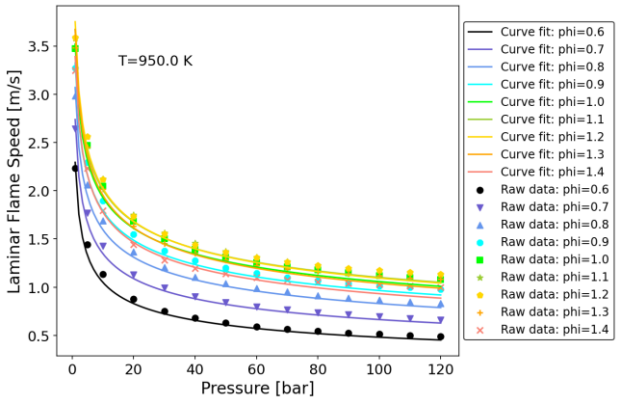

Fig. 10 Predicted laminar flame speed using the improved Arrhenius form correlations with different pressures and equivalence ratios at 950 K: curves for correlations and points for the LLNL detailed kinetics simulations.

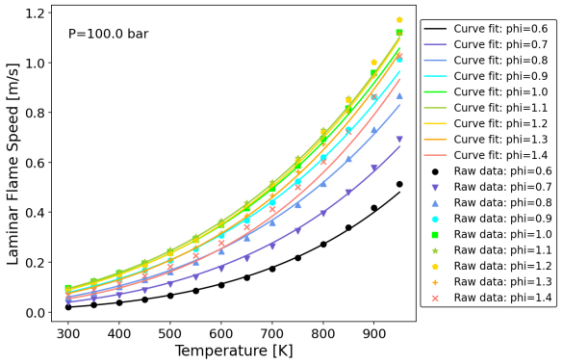

Fig. 11 Predicted laminar flame speed using the improved Arrhenius form correlations with different temperatures and equivalence ratios at 100 bar; curves for correlations and points for the LLNL detailed kinetics simulations.

DISCUSSION

Correlations for a Narrow Range of Conditions

As mentioned earlier, the improved power law form fails to predict the temperature dependence very accurately for a wide range of conditions. Besides, from the pressure dependence plots (Fig. 6 and Fig. 10), the curves are very steep for the low-pressure ranges, so it is always a concern whether the improved correlation can provide accurate predictions for different pressure ranges at the same time. Thus, to present better predictions, curve fits are repeated using the same methods, while this time, the operating conditions focus on a narrow range: 300-700 K for the unburned temperature, 1-12 bar for pressure, and 0.6-1.4 for equivalence ratio. The corresponding coefficients are shown in Table 5 and Table 6.

Table 5 Coefficients for α (Eqn. (13)) and β (Eqn. (14)) (A denotes A_0 when $\phi < \phi_m$, and denotes A_1 when $\phi > \phi_m$; the same for B & C) for laminar flame speed fits (Eqn. (10)) using the power law method derived for a narrow range of conditions.

Coef.	A	B	C	D
α	13.6915	1.0313	3.6670	1.8562
β	A	B	C	
	$\phi < \phi_m$=1.12			
	-0.4887	0.9715	-0.7722	
	$\phi > \phi_m$=1.12			
	-0.8754	1.8377	-1.2573	

Table 6 Coefficients (A denotes A_0 when $\phi < \phi_m$, and denotes A_1 when $\phi > \phi_m$; the same for B & C) for α, β, and γ (Eqn. (21)) in the improved Arrhenius form correlations (Eqn. (20), U = 4300) derived for a narrow range of conditions.

Coef.	ϕ_m=1.12	A	B	C
α	$\phi < \phi_m$	-0.5869	1.1508	-0.8402
β		-76622	150405	-31486
γ		-9393	18840	-5284
α	$\phi > \phi_m$	-0.6898	1.3814	-0.9694
β		-85514	170324	-42641
γ		-11409	23356	-7813

It turns out that both the improved power law form and the improved Arrhenius method can provide good predictions for the narrow range mentioned earlier. For the sake of brevity, the predicted results using only the improved power law method for the narrow range are shown in Fig. 12 and Fig. 13. The corresponding fit errors will be shown as well in the next section.

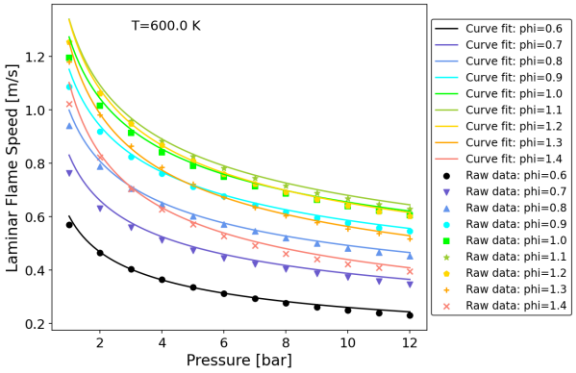

Fig. 12 Predicted laminar flame speeds using the improved power law correlations derived for a narrow range: temperature is fixed at 600 K; curves for correlations and points for simulated results.

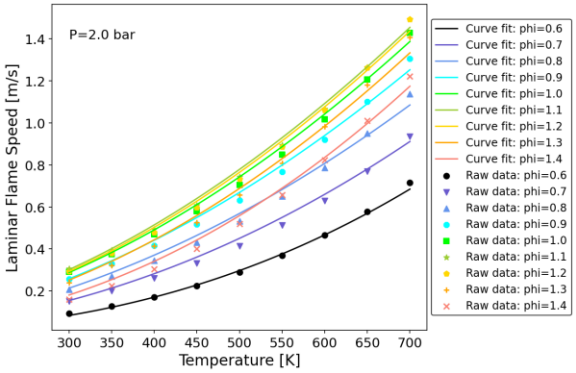

Fig. 13 Predicted laminar flame speeds using the improved power law correlations derived for a narrow range: pressure is fixed at 2 bar; curves for correlations and points for simulated results.

Comparisons Between the Two Correlations

The standard errors for the fits using both the improved power law method and the improved Arrhenius form method were calculated, using Eqn. (23).

$$\Delta S_L = \sqrt{\frac{\sum\left(\widehat{S_{Li}} - S_{Li}\right)^2}{n - K}} \qquad (23)$$

where $\widehat{S_{Li}}$ is the predicted laminar flame speed using the improved correlations, and S_{Li} is the original simulated result from the LLNL detailed kinetics; K is the number of parameters in the regression and n - K is the number of degrees of freedom of the regression.

The standard errors for the two methods are shown in Table 7. It can be seen that the improved power law method has more than twice the error in both ranges of operating conditions compared to the improved Arrhenius form method, indicating the latter method is a better

representation of the original detailed LLNL kinetics simulation results.

Table 7 Standard errors for the fits using the improved methods.

Operating conditions	Fit method	Errors [cm/s]
Wide range	Improved power law	7.67
	Improved Arrhenius form	3.20
Narrow range	Improved power law	3.17
	Improved Arrhenius form	1.58

Comparisons Between the Original and Improved Correlations

Power Law Form

As mentioned earlier, one of the best known studies using the power law form correlations is the work by Metghalchi and Keck [6,7]. They concluded that the three coefficients (S_{Lo}, α, and β in Eqn. (10)) could be represented by Eqns. (24), (25), and (26):

$$S_{L0} = B_m + B_2(\phi - \phi_m)^2 \quad (24)$$

$$\alpha = 2.18 - 0.8(\phi - 1) \quad (25)$$

$$\beta = -0.16 + 0.22(\phi - 1) \quad (26)$$

They found that the temperature and pressure exponents, α and β, were independent of fuel type (methanol, propane, iso-octane, and indolene), so they could be represented by the same linear form function of equivalence ratio. However, the linear form was obtained using only three different equivalence ratios (ϕ = 0.8, 1.0, and 1.2), and they did not include any data points in the very lean or rich regions.

For the baseline S_{Lo} expression, they used a 2nd order polynomial form, with $\phi = \phi_m$ as the axis of symmetry, but there is no reason for S_{Lo} to be symmetric about ϕ_m, especially since they found ϕ_m from a 2nd order fit to only 3 data points. Again, only three equivalence ratios were used around the stoichiometric condition in their study, so their fits for the unstretched laminar flame speed at 298.15 K and 1 atm, S_{Lo}, matched their measurements well.

Shown in the present study, the power law form correlation is valid when the temperature and pressure range is not too large. Although the curve fits in the present study for these three coefficients look a little more complicated than Metghalchi and Keck's, they do yield very good results, shown in Fig. 12 and Fig. 13.

Arrhenius Form

There are two main difficulties [7,13] when using the original Arrhenius form correlations (Eqn. (15) or (16)). First, the Arrhenius form is very sensitive to the flame temperature, T_f, which is in turn sensitive to the thermodynamic model used to calculate it. Second, the parameters in the original Arrhenius form vary erratically with equivalence ratio, probably because T_f peaks at a different equivalence ratio from S_L, which makes it very difficult to get a smooth and simple curve fit.

Using the algorithm proposed in the "Improved Arrhenius Form" section of this research, calculating T_f is not a concern, since it is replaced by a function of T_u. Also, after doing that, the pre-exponential factor U is estimated as a constant value and all the other coefficients can be represented using a simple function of equivalence ratio. This solves the problem mentioned above and makes the improved Arrhenius method suitable for practical use. More importantly, the improved Arrhenius form halves the overall fit error (Table 7) and thus is a better approach compared to the improved power law method.

Comparisons with Other Studies

Different measurements of the laminar flame speed for iso-octane have been made in several studies (e.g., Liao and Roberts [18], Huang et al. [19], Sileghem et al. [20], Kumar et al. [21], Jerzembeck et al. [22], and Mannaa et al. [23]). The LFS results, obtained using the two improved correlations proposed in the present study are compared with those measurements over a range of unburned gas temperatures, pressures, and equivalence ratios in Fig. 14, where the green solid curve represents the results calculated based on the improved power law method, the blue solid curve represents the results using the improved Arrhenius method, and all the other points with different colors show the experimental measurements by the various researchers mentioned above. The parameters obtained for the narrow range were used in the improved correlations for the low pressures in Fig. 14a and b, and those for the wide range were used for the high pressures in Fig. 14c and d.

First, the predicted ϕ_ms using both improved correlations match well with the measurements. Second, the LFS predictions using the improved Arrhenius method agree quite well under all these conditions including a range of unburned temperatures, pressures, and equivalence ratios. Third, although it was stated that the power law correlations failed to predict the speeds accurately for a wide range of conditions, the deviations from the experiments are still not huge. Finally, the power law predictions are always higher than the Arrhenius form predictions under the conditions compared, because these temperatures are not very high and the improved power law method always overestimates the results under these conditions, as shown in Fig. 7.

Shown together in Fig. 14 are two dashed curves, which are the predicted results using two other correlations for iso-octane from Metghalchi and Keck [7] (Metghalchi's correlation, grey curves) and Marshall et al. [24] (Marshall's correlation, orange curves). It was stated in Marshall's paper that their maximum experimental pressure for iso-octane was 600 kPa, so Marshall's correlation is not shown in the 20 bar and 25 bar comparisons. It is seen in Fig. 14a that Metghalchi's correlation is close to the improved correlation in this research and the experimental points, while Marshall's correlation underestimates the values for most equivalence ratios at room temperature and pressure. The reason is that Marshall et al. stated in their paper that their correlation for iso-octane was valid for the temperature range of 340-640 K based on their measurements, which is higher than the temperature in Fig. 14a. Both Metghalchi's correlation in Fig. 14b, c, and d,

and Marshall's correlation in Fig. 14b show reasonable predictions for the lean region, while the predictions get worse when the mixture becomes rich. The possible explanations are: for Metghalchi's correlation, again, only three equivalence ratios around 1.0 were used to derive the correlation; for Marshall's correlation, as stated in their paper, there were far fewer valid experimental data points at high equivalence ratios, so the correlation became biased towards lower equivalence ratios.

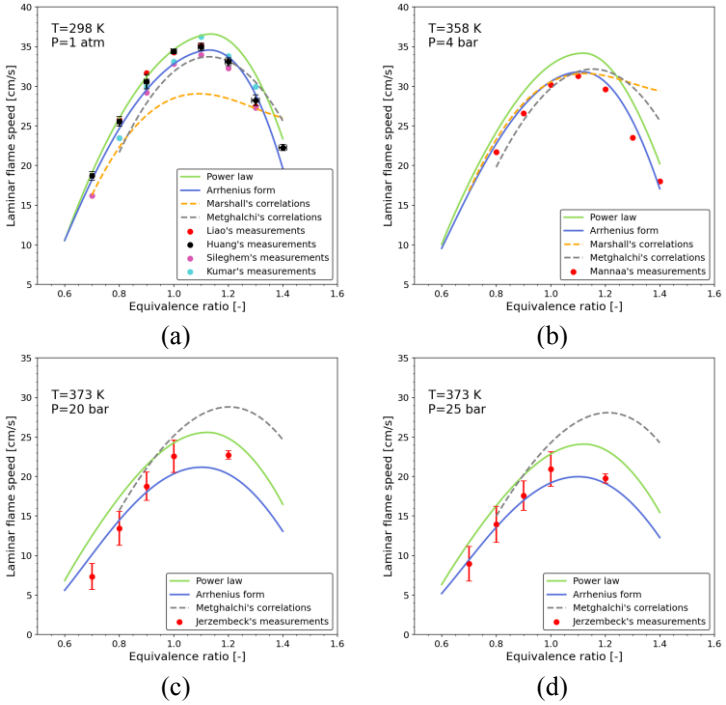

Fig. 14 Laminar flame speed comparisons between experimental measurements (dots) from various papers, correlations (dashed curves) from other studies and both improved correlations (solid curves) from the present study: (a) room temperature and 1 atm; (b) 358 K and 4 bar; (c) 373 K and 20 bar; (d) 373 K and 25 bar.

Published data remains scarce for the high-temperature and high-pressure conditions; more measurements are needed to show the validity of both improved correlations for elevated conditions, especially for pressures over 100 bar. However, from the existing measurements, both improved correlations are able to predict the unstretched laminar flame speeds quite well for engineering design and analysis. In particular, the improved Arrhenius form correlation is recommended for use over the improved power law method, considering its excellent predictions over all the temperature, pressure, and equivalence ratio ranges covered in this paper.

SUMMARY AND CONCLUSIONS

Two improved correlations for the laminar flame speed, an improved power law correlation and an improved Arrhenius form correlation, are proposed for iso-octane in this study based on CONVERGE one-dimensional simulation results using the LLNL reaction mechanism. The typical working conditions for a spark-ignition engine, 300-950 K for unburned temperature, 1-120 bar for pressure, and 0.6-1.5 for equivalence ratio, were chosen to generate the results. Each of the two improved correlations has three parameters to be determined and these parameters are all shown as simple functions of equivalence ratio. The predicted unstretched laminar flame speeds using these two correlations were compared with the experimental measurements and the other correlations from various researchers.

1. The ϕ_m and LFS_m were investigated first. It turned out ϕ_m was a relatively weak function of temperature and pressure, and it ranged around 1.10-1.20 under different conditions (we will attempt to obtain a better correlation for ϕ_m over the full ranges of T and P by the time this paper is presented.). The correlations for ϕ_m (a relatively narrow range) and LFS_m are given. ϕ_m is of practical interest because it corresponds to the equivalence ratio that yields least-rich best torque (LBT) and LFS_m is the unstretched laminar flame speed at this condition.

2. Two continuous parabolic functions were used to represent S_{Lo} and β in the improved power law form correlation for laminar flame speed, and a power relation was used to represent the other coefficient α.

3. A linear correlation with T_u was used to represent T_b, to make the improved Arrhenius form easier to use than the original one. It turned out the pre-exponential factor in the improved Arrhenius form correlation did not vary a lot with different conditions and was assumed as a constant value. Similar to S_{Lo}, a piecewise parabolic function was used to represent each of the other three coefficients.

4. The results at ϕ=1.5 were not included in the above correlations, since a different trend was seen for the very rich mixture.

5. Comparisons with others' experimental results indicated reasonable predictions using both improved

correlations. The improved Arrhenius form correlation was closer to the experimental measurements, while the improved power law correlation overestimated the results for the conditions shown. Besides, the standard error of the fits for the improved Arrhenius form correlation was about half of that for the improved power law correlation, which indicated better predictions using the improved Arrhenius method as well.

In summary, both improved correlations, using simple and workable expressions, were able to predict the trends and the values of the unstretched laminar flame speed with improved accuracy. The improved Arrhenius form was more accurate and presented good predictions over a large range of operating conditions, and therefore is recommended for practical calculations and predictions. The two correlations are summarized in Table 8 for the reader's convenience.

Table 8 Summary of the improved power law and improved Arrhenius form correlations: the improved Arrhenius form is recommended; the coefficients for the narrow range are preferred if the target condition is within the narrow range; the unit for the calculated LFS is m/s.

Correlations	Improved power law	Improved Arrhenius form
Conditions	Narrow: T, 300-700 K; P: 1-12 bar; ϕ, 0.6-1.4. Wide: T, 300-950 K; P: 1-120 bar; ϕ, 0.6-1.4.	
Expressions	S_L: Eqn. (10) S_{Lo}: Eqn. (11) α: Eqn. (13) β: Eqn. (14)	S_L: Eqn. (20) α, β, and γ: Eqn. (21)
Coefficients	S_{Lo}: Table 2 α and β: Table 5 for narrow; Table 3 for wide.	U: 4300 for narrow; 4100 for wide. α, β, and γ: Table 6 for narrow; Table 4 for wide.

Acknowledgements

This project was made possible through funding provided by Ford through the University of Texas at Austin's site of the NSF Center for Efficient Vehicles and Sustainable Transportation Systems (EVSTS). We also wish to thank CONVERGE CFD™ for providing us with licenses for their simulation software and for their generous technical support. We also thank Dr. Terry Alger and Dr. Robbie Mitchell of Southwest Research Institute for providing the peak pressure and unburned gas temperature extremes for a TGDI engine at full load.

NOMENCLATURE

LBT: Least-rich best torque
LFS: Laminar flame speed (unstretched)
MON: Motor Octane Number
PRF: Primary reference fuel
RON: Research Octane Number
SI: Spark ignition
TRF: Toluene reference fuel
ϕ: Equivalence ratio
Subscript
m: Maximum or that yields the maximum LFS

REFERENCES

[1] Gouldin, F.C., *Combust. Flame* 68(3):249–266, 1987.
[2] Matthews, R.D., Hall, M.J., Dai, W., and Davis, G.C., *SAE Journal of Engines* 105:180–195, 1996.
[3] Egolfopoulos, F.N., Hansen, N., Ju, Y., Kohse-Höinghaus, K., Law, C.K., and Qi, F., *Progress in Energy and Combustion Science* 43:36–67, 2014.
[4] Pires Da Cruz, A., Dean, A.M., and Grenda, J.M., *Proceedings of the Combustion Institute* 28(2):1925–1932, 2000.
[5] Syed, I.Z., Yeliana, Mukherjee, A., Naber, J.D., and Michalek, D., *SAE International Journal of Engines* 3(1):517–528, 2010.
[6] Metghalchi, M. and Keck, J.C., *Combust. Flame* 38:143–154, 1980.
[7] Metghalchi, M. and Keck, J.C., *Combust. Flame* 48:191–210, 1982.
[8] Bozza, F., De Bellis, V., Giannattasio, P., Teodosio, L., and Marchitto, L., *SAE International Journal of Engines* 10(4):2141–2153, 2017.
[9] Adamo, A. d', Del Pecchia, M., Breda, S., Berni, F., Fontanesi, S., and Prager, J., SAE Paper 2017-01-2190, 2017.
[10] Lavoie, G.A., *SAE Transactions* 87:1015–1033, 1978.
[11] Ryan, T.W. and Lestz, S.S., *SAE Transactions* 89:652–664, 1980.
[12] Gülder, Ö.L., SAE Paper 841000, 1984.
[13] Amirante, R., Distaso, E., Tamburrano, P., and Reitz, R.D., *International Journal of Engine Research* 18(9):951–970, 2017.
[14] Mehl, M., Pitz, W.J., Sjöberg, M., and Dec, J.E., SAE Paper 2009-01–1806, 2009.
[15] Mehl, M., Curran, H.J., Pitz, W.J., and Westbrook, C.K., Lawrence Livermore National Lab.(LLNL), Livermore, CA (United States), 2009.
[16] Curran, H.J., Gaffuri, P., Pitz, W.J., and Westbrook, C.K., *Combust. Flame* 129(3):253–280, 2002.
[17] Semenov, N.N., NACA-TM-1026, 1942.
[18] Liao, Y.-H. and Roberts, W.L., *Energy Fuels* 30(2):1317–1324, 2016.
[19] Huang, Y., Sung, C.J., and Eng, J.A., *Combust. Flame* 139(3):239–251, 2004.
[20] Sileghem, L., Alekseev, V.A., Vancoillie, J., Van Geem, K.M., Nilsson, E.J.K., Verhelst, S., and Konnov, A.A., *Fuel* 112:355–365, 2013.
[21] Kumar, K., Freeh, J.E., Sung, C.J., and Huang, Y., *Journal of Propulsion and Power* 23(2):428–436, 2007.
[22] Jerzembeck, S., Peters, N., Pepiot-Desjardins, P., and Pitsch, H., *Combust. Flame* 156(2):292–301, 2009.
[23] Mannaa, O., Mansour, M.S., Roberts, W.L., and Chung, S.H., *Combust. Flame* 162(6):2311–2321, 2015.
[24] Marshall, S.P., Taylor, S., Stone, C.R., Davies, T.J., and Cracknell, R.F., *Combust. Flame* 158(10):1920–1932, 2011.